Journal of Thermal Analysis and Calorimetry, Vol. 89 (2007) 1, 303–307

CALORIMETRIC SEARCH FOR THE DISCONTINUITY IN $Fe_{0.96}S$–$Ni_{0.96}S$ SOLID SOLUTIONS

V. A. Drebushchak[1,2*] *and E. F. Sinyakova*[1]

[1]Institute of Mineralogy and Petrography, Siberian Branch of the Russian Academy of Sciences, pr. Koptyuga, 3, Novosibirsk 630090, Russia
[2]Research and Education Center 'Molecular Design and Ecologically Safe Technologies', REC-008, Novosibirsk State University, ul. Pirogova, 2, Novosibirsk 630090, Russia

Heat capacity of unstable quenched solid solutions $(Fe_{1-x}Ni_x)_{0.96}S$ was measured by DSC (enthalpy method and scanning heating). According to optic microscopy and X-ray powder diffraction, the samples are homogeneous phase of NiAs type with unit cell parameters changing regularly with composition.

Heat capacity changes with composition irregularly due to the difference in magnetic properties of the end members: $C_p/1.96R$=4.1 for Fe-rich samples and 3.3 for Ni-rich ones. There is no exact limit between two types of magnetic ordering. Instead, samples with intermediate composition ($0.7<x<0.8$) show large fluctuations in C_p due to the inconsistency of alternative (FeS and NiS) types of magnetic ordering.

Keywords: *DSC, Fe–Ni–S system, heat capacity, magnetic contribution, solid solutions, stability*

Introduction

Monosulfide solid solutions (*mss*) $Fe_{1-x}S$–$Ni_{1-x}S$ are common in metallurgical processes [1–3] and natural sulfide ores [4–8]. Synthesized at high temperatures, the homogeneous phases are stable at temperatures above 600°C. If cooled down to room temperature slowly, the *mss* decay into two phases: pentlandite $(Fe,Ni)_{9.14}S_8$ and Fe-enriched *mss* [9]. Quenched into water, the *mss* remain homogeneous at room temperature for indefinitely long time. Again, the quenched *mss* decay into pentlandite and Fe-enriched *mss* if heated above 220°C. We investigated the decay of the metastable samples by means of DSC and X-ray powder diffraction [10]. Inconsistency between magnetic structures of the end-member phases was suggested to be the reason of the decay of intermediate *mss*. At room temperature, there is magnetic order in FeS, but not in NiS.

Unit cell parameters of the quenched *mss* vary regularly with the Fe/Ni ratio and does not reveal any discontinuity [10]. It is not surprising fact because even drastic changes in magnetic or ferroelectric ordering, exibiting themselves as the second-order [11] or first-order phase transitions [12], cannot be detected in the unit cell parameters sometimes. Synchrotron radiation S K-edge XANES spectra of the *mss* also show regular changes in the energy of interaction between atoms, without any discontinuity [13].

Our attempt to investigate directly the magnetic properties (magnetic susceptibility) of the *mss* has failed. The readings were found to change significantly during the experiments under variable magnetic field and/or temperature (Drebushchak and Kuropyatnik, unpublished). Such an investigation turned out to deal with the kinetics of the transformation in the magnetic ordering under diffusion of magnetic ions in a solid, but not with the magnetic state itself. High mobility of Fe and Ni atoms in the *mss* near 100°C was proved by DSC and X-ray powder diffraction [14].

Magnetic ordering in a phase produces a contribution into its heat capacity. Differences in the magnetic properties of the crystals even with the same structure must result in the differences in their heat capacities.

The objective of this work was to measure the heat capacity of quenched samples of the *mss*. Discontinuity in the relationship between C_p and Fe/Ni ratio can indicate the limits in the composition of the *mss* with identical type of magnetic ordering. This, in turn, can either support or reject the hypothesis about the key role of the inconsistency in the magnetic structures of end-member phases in the instability of *mss* with intermediate composition.

Experimental

Eleven quenched samples with the composition of $(Fe_{1-x}Ni_x)_{0.96}S$ (x=0, 0.1,..., 1) were synthesized from reagents Fe, Ni, and S of high-purity grade. The charges were sealed in an evacuated silica tube,

* Author for correspondence: dva@uiggm.nsc.ru

1388–6150/$20.00

Akadémiai Kiadó, Budapest, Hungary
Springer, Dordrecht, The Netherlands

heated up to the melting, kept at 900°C for 12d, and then dropped into water at room temperature. The quenched samples were analyzed by optic microscopy and X-ray powder diffraction and found to be homogeneous crystalline solid solutions with the hexagonal unit cell.

Two types of calorimetric measurements were carried out: (1) scanning heating at a heating rate of 3 K min^{-1} using DSC-30 of the Mettler TA-3000 System and (2) step heating (enthalpy method) using DSC-111 Setaram.

In the scanning heating measurements, the reproducibility of the results was estimated after eight series of blank runs and the standard deviation of the DSC signal turned out to be of 0.13 mW at 400 K. Sample masses ranged from 65 to 85 mg, and the irreproducibility in the DSC signal produces the standard deviation in C_p of 0.03–0.04 J g^{-1} K^{-1}. All synthesized *mss* samples were measured in the scanning heating mode.

The DSC-111 was calibrated against α-Al_2O_3. All the step heating measurements were carried out using only one aluminum crucible. The accuracy of the measurements was about 1%. In general, very accurate measurements are optional for the evaluation of thermodynamic functions of quenched samples because unstable phases are not quite suitable object for careful thermodynamic investigations, but the objective of this work does need very accurate data on C_p. In the step-heating experiments only samples with x=0, 0.1, 0.2, 0.8, 0.9 and 1 were investigated. Samples with x=0, 0.1, 0.8, 0.9 and 1 do not exsolve pentlandite during the experiments with certainty, remaining homogeneous even after the slow cooling down to room temperature. Sample with x=0.2 remains homogeneous after the heating up to 580 K. The sample masses were 680.96, 743.88, 792.01, 820.50, 909.05 and 793.05 mg for x=0, 0.1, 0.2, 0.8, 0.9 and 1, respectively. In the step heating experiments, the temperature increment of 10 K was used. The measurements were repeated with the temperature increment of 3 (x=0.1, 0.9 and 1) or 4 K (x=0.8), over a temperature range where the phase transition takes place.

X-ray powder diffraction (XRD) experiments were carried out using diffractometer DRON-3. The experiments were performed according to the recommendation of the International Center for Diffraction Data and three of eleven XRD patterns were included into the ICDD database: entries 50-1788 ($Fe_{0.96}S$), 50-1789 ($Fe_{0.48}Ni_{0.48}S$), and 50-1791 ($Ni_{0.96}S$).

Results and discussion

The results of the step-heating measurements are listed in Table 1. Unsmoothed experimental values allow one to make sure that the heat capacities reproduce very well both within one run and among different series. All the samples undergo the phase transition at temperatures near 350 K. Step heating is not quite suitable way for calorimetric measurements of such a phenomenon because the heat effect that accompanies the transformation is smeared in time, and the measured heat flow during the transition relaxes very slowly, corrupting the baseline and increasing inaccuracy. In investigating the 'regular' heat capacity rather than the peak of the transition, we applied special procedure for the accurate measurements. As the inverse phase transition at room temperature (i.e., from high-temperature to low-temperature state after the cooling) needs a time to allow the sample to return back into the starting state, immediate start of the second run just after the cooling keeps the sample in the high-temperature state. At the second heating, the phase transition was not detected for the samples with x=0.1 and 0.9, and only the regular heat capacity was measured. For the sample with x=1, small peak of the phase transition repeated. For the sample with x=0.8, large peak of the phase transition was measured at the second heating, that will be discussed below.

For all the substances, heat capacity is a smooth function of temperature above 390 K. We chose the point T=400 K to search for the changes in the heat capacities of the solid solutions. The heat capacity derived from the scanning heating experiments is nearly constant within the limits of experimental error for the samples with x ranging from 0 to 0.6, and close to the values measured by step heating. It is evidently less for x=0.8, 0.9 and 1, both for step and scanning heating. For x=0.7, the heat capacity is extremely large. The results for the sample with x=0.7 were found to be irreproducible. Figure 1 shows the results after three runs, one at 3 and two at 5 K min^{-1}. There are the peaks, 'regular' heat capacities, and heat release in the curves. The values of 'regular' heat capacity differ as much as 50% near T=400 K.

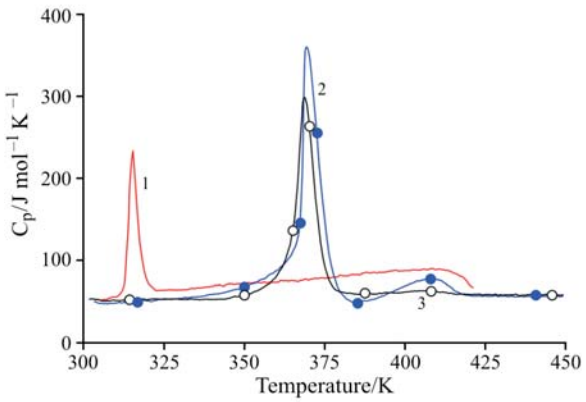

Fig. 1 Irreproducibility of DSC results at scanning heating for the *mss* with x=0.7. First run at 1 – 3 K min^{-1}, 2 – second run at 5 K min^{-1} and 3 – third run at 5 K min^{-1}

Table 1 Experimental heat capacities of the *mss*

T/K	C_p/J g^{-1} K^{-1}	T/K	C_p/J g^{-1} K^{-1}	T/K	C_p/J g^{-1} K^{-1}	T/K	C_p/J g^{-1} K^{-1}	T/K	C_p/J g^{-1} K^{-1}
x=0		364.5	0.749	349.6	0.631	323.2	0.579	364.5	0.621
314.8	0.647	374.4	0.753	353.5	0.562	326.2	0.587	374.4	0.645
374.4	1.398	384.3	0.757	357.5	0.551	329.2	0.591	384.3	0.604
384.3	0.775	394.3	0.763	364.5	0.551	332.2	0.594	394.3	0.607
394.3	0.776	404.2	0.767	374.4	0.550	335.2	0.595	404.2	0.610
404.2	0.776	414.1	0.767	384.3	0.551	338.1	0.598	414.1	0.610
414.1	0.780	424.1	0.770	394.3	0.551	341.1	0.593	424.1	0.615
424.1	0.779	434.0	0.774	404.2	0.551	344.1	0.597	404.2	0.607
434.0	0.789	444.0	0.778	414.1	0.550	347.1	0.596	414.1	0.608
404.2	0.778	x=0.2		424.1	0.551	350.1	0.598	424.1	0.614
414.4	0.780	334.7	0.710	434.0	0.552	353.0	0.600	434.0	0.617
424.1	0.783	344.6	0.722	444.0	0.551	356.0	0.597	444.0	0.623
434.0	0.788	354.5	0.728	x=0.9		359.0	0.604	344.1	0.583
444.0	0.790	364.5	0.739	314.8	0.573	362.0	0.598	347.1	0.586
453.9	0.789	374.4	0.748	324.7	0.583	365.0	0.600	350.1	0.592
463.8	0.800	384.3	0.755	334.7	0.591	367.9	0.601	353.0	0.595
473.8	0.790	394.3	0.763	344.6	0.598	370.9	0.603	356.0	0.600
483.7	0.811	404.2	0.768	374.4	0.643	373.9	0.603	359.0	0.605
493.6	0.824	414.1	0.774	384.3	0.606	376.9	0.603	362.0	0.613
x=0.1		424.1	0.784	394.3	0.608	379.9	0.605	365.0	0.616
314.8	0.682	434.0	0.790	404.2	0.607	382.8	0.605	367.9	0.624
324.7	0.727	444.0	0.798	414.1	0.609	385.8	0.604	370.9	0.633
331.2	0.732	453.9	0.802	424.1	0.611	388.8	0.607	373.9	0.642
334.2	0.736	463.8	0.815	434.0	0.615	391.8	0.609	376.9	0.642
337.1	0.736	473.8	0.821	444.0	0.618	394.8	0.615	379.9	0.613
340.1	0.740	x=0.8		453.9	0.617	397.7	0.611	382.8	0.602
343.1	0.739	313.8	0.511	463.8	0.619	x=1		385.8	0.600
346.1	0.736	317.8	0.518	473.8	0.619	314.8	0.570	388.8	0.602
349.1	0.739	321.7	0.529	483.7	0.621	324.7	0.575	391.8	0.601
352.0	0.741	325.7	0.540	314.3	0.569	334.7	0.586	394.8	0.604
355.0	0.745	329.7	0.557	317.3	0.573	344.6	0.589	397.7	0.604
358.0	0.747	333.7	0.578	320.2	0.582	354.5	0.601		

At the same time, one should point out that the sample remains homogeneous after experiments and long storage at room temperature. During the second run at a heating rate of 5 K min^{-1} the heat capacity at 400 K was 62 J mol^{-1} K^{-1}. This is close to the values of 66.6, 65.9 and 66.5 J mol^{-1} K^{-1} measured with step heating for the solid solutions with x=0, 0.1 and 0.2, respectively.

Heat capacity as a function of composition

To compare the heat capacities of substances varying in formula mass and in the number of atoms in the formula, it is necessary to recalculate the experimental values into the degrees of freedom. For the $Fe_{0.96}S$–$Ni_{0.96}S$ solid solutions, it is $C_p/1.96/R$, where R is the gas constant. The results are shown in Fig. 2. Heat capacities of iron-rich solid solutions are greater than those of nickel-rich samples by about one degree of freedom. This difference is nearly equal to the change in the heat capacity when an iron-rich solid solution undergoes phase transition into paramagnetic state [10]. Heat capacity of *mss* with x=0.8 is equal to the classical value C_p=3R (Dulong–Petit). For pyrrhotites with various metal-to-sulfur ratios, the numbers of degrees of freedom are 4.21 (FeS [15]), 3.67 ($Fe_{0.9}S$ [16]), 3.65 ($Fe_{0.89}S$ [15]), and 3.56 ($Fe_{0.875}S$ [15]). Pyrrhotite with composition $Fe_{0.98}S$ in [15] is most close to our *mss* in the metal-to-sulfur ratio, but it has the phase transition near 400 K. Heat capacity decreases after the phase transition, reaching the least value at 440 K and then grows

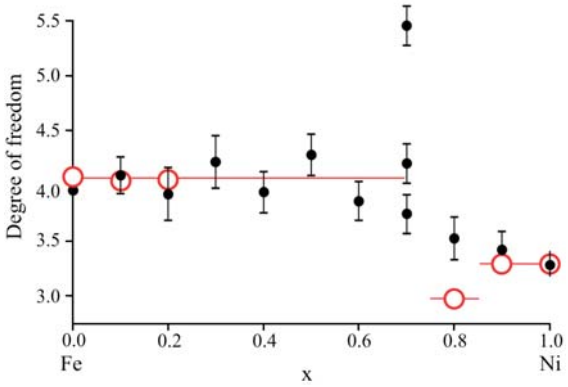

Fig. 2 Number of the degrees of freedom in the heat capacity of *mss* as a function of the Fe/Ni ratio. The standard deviations of the results of enthalpy method are less than the size of marks (open circles). Results of scanning heating (filled circles) for the sample with x=0.7 are shown for three runs (Fig. 1)

again. For 440 K, $Fe_{0.98}S$ has 4.10 degrees of freedom. Figure 2 shows that the regular heat capacities at 400 K are nearly constant for the *mss* with $0 \le x \le 0.6$ at constant metal-to-sulfur ratio of 0.96.

In considering the changes in the heat capacity of nonstoichiometric ternary solid solutions $(Fe_{1-x}Ni_x)_{1-y}S$ caused by the changes in the Fe-to-Ni and metal-to-sulfur ratios, one can distinguish the effects of the metal substitution (x) and vacancies (y). Both vacancies and nickel atoms act as defects in the magnetic lattice formed by Fe atoms in pyrrhotite, but the vacancies change 'regular' heat capacity and the nickel atoms do not.

Heat capacity of NiS was discussed in [17]. The careful measurements of a synthetic sample show that its heat capacity depend on thermal history. At heating started from 260 K, stoichiometric NiS can behave either like stable phase 'millerite' or like unstable phase of NiAs-type. The latter transforms exothermally into stable 'millerite' at temperatures above 340 K [17]. It is interesting that the heat capacities of metastable and stable phases of stoichiometric NiS are close to those of the solid solutions with x=1, 0.9 and x=0.8, respectively. Such a similarity is not quite understood. In considering chemical composition, the *mss* with x=1 and 0.9 are much alike to stoichiometric NiS than that with x=0.8 and they must be evidently much stable than the latter. Nevertheless, this is the fact that the monosulfide solid solution with x=0.8 differ in heat capacity from those with x=1 and 0.9 as if their structures differ drastically: millerite is rhombohedral (hexagonal unit cell with a=0.96 nm, c=0.315 nm) and NiAs-type phase is hexagonal (a=0.34 nm, c=0.535 nm). At the same time, no such a difference in structure is observed in the series of *mss*. Unit cell parameters derived from XRPD patterns for the whole series of the *mss* are listed in Table 2. For eight peaks, their interplanar spacing and amplitude are indicated. First of all, it is evident from the table that no drastic change in the structure of the solid solutions takes place when the composition changes from $Fe_{0.96}S$ to $Ni_{0.96}S$. The indexes for all the samples are based on the hexagonal unit cell of NiAs-type. It is not surprising that the *mss* with $0 \le x \le 0.8$ are of the NiAs-type. The heat capacity of the *mss* with $x \le 0.7$ is similar to that of pyrrhotite which in turn is of NiAs-type. The heat capacity of the *mss* with x=0.8 is close to that of the unstable NiS phase which is of NiAs-type too. It is very surprising that the *mss* with x=0.9 and 1 have the heat capacity similar to that of stable millerite but the structure similar to the NiAs-type. The only evident difference between XRD patterns of the *mss* with $x<0.85$ and $x>0.85$ is the highest peak: (100) for $Ni_{0.96}S$ instead of (102) for $Fe_{0.96}S$. Unit cell parameters (a, b, c, α, β, γ) and the interplanar distances (d) characterize the geometry of a structure, i.e., the positions of atoms. These change regularly with the Fe-to-Ni ratio in the quenched *mss*. The intensity of a reflection (I) de-

Table 2 XRD data (d/I) for monosulphide solid solutions

Solid solution	Reflections h k l							
	1 0 0	0 0 2	1 0 1	1 0 2	1 1 0	1 0 3	2 0 0	2 0 1
$Fe_{0.96}S$	2.98/51	2.903/8	2.652/56	2.083/100	1.722/34	1.624/6	1.492/2	1.452/5
$(Fe_{0.9}Ni_{0.1})_{0.96}S$	2.985/44	2.869/5	2.648/50	2.069/100	1.724/31	1.611/7	1.492/2	1.445/4
$(Fe_{0.8}Ni_{0.2})_{0.96}S$	2.98/46	2.856/6	2.644/46	2.064/100	1.722/30	1.607/4	1.491/3	1.444/4
$(Fe_{0.7}Ni_{0.3})_{0.96}S$	2.98/51	2.842/6	2.640/52	2.057/100	1.722/35	1.599/6	1.491/3	1.442/5
$(Fe_{0.6}Ni_{0.4})_{0.96}S$	2.98/57	2.822/5	2.637/50	2.050/100	1.721/35	1.592/6	1.490/3	1.441/4
$(Fe_{0.5}Ni_{0.5})_{0.96}S$	2.98/86	2.805/4	2.635/66	2.043/100	1.722/53	1.581/4	1.490/5	1.441/5
$(Fe_{0.4}Ni_{0.6})_{0.96}S$	2.98/50	2.774/3	2.626/40	2.033/100	1.719/31	1.571/4	1.488/3	1.438/4
$(Fe_{0.3}Ni_{0.7})_{0.96}S$	2.98/80	2.763/6	2.622/50	2.025/100	1.720/40	1.566/6	1.490/3	1.439/4
$(Fe_{0.2}Ni_{0.8})_{0.96}S$	2.98/77	2.747/6	2.613/69	2.020/100	1.718/77	1.559/7	1.489/7	1.437/8
$(Fe_{0.1}Ni_{0.9})_{0.96}S$	2.98/100	2.678/2	2.603/37	1.993/52	1.717/70	1.529/4	1.485/5	1.432/4
$Ni_{0.96}S$	2.97/100	2.667/4	2.600/51	1.986/75	1.717/52	1.523/5	1.485/5	1.430/5

pends on the spatial electron density distribution, and the functional relation can be very complicated for new materials with unusual properties, e.g., for stoichiometric superionics [18]. The intensities turned out to change evidently and we can deduce that the electron density distribution changes as well.

Limit between Fe- and Ni-rich mss

In the previous report we defined the least value for the Fe content of the *mss* when the quenched sample decays at heating, exsolving pentlandite [10]. It was the estimate of the discontinuity border for the solid solutions. Investigating the heat capacity of the *mss* in this work, we can search for the border more accurately. According to the heat capacity values, the sample $(Fe_{0.2}Ni_{0.8})_{0.96}S$ belongs neither $Fe_{0.96}S$-type nor $Ni_{0.96}S$-type. Again, the irreproducibility in the heat capacity of $(Fe_{0.3}Ni_{0.7})_{0.96}S$ shows the instability of the sample. Probably, neither of two competing phases with different electronic structures has the preference in the range of $0.7 \le x \le 0.8$.

One can conclude that there is no single border value for the composition of the *mss*, but the region with strong fluctuations in the electronic structure of intermediate compositions. In our investigations, the temperature of magnetic transition, enthalpy, and heat capacity of the *mss* with x=0.7 change drastically after heating–cooling cycles, but no changes in its composition were detected, and the sample remains homogeneous and crystalline. The heat capacity of the *mss* with x=0.8 turned out to be different from both end-member phases, neither FeS nor NiS. Contrary to other *mss*, that sample showed large peak of the phase transition near 350 K at the second run in the step-heating experiments.

Conclusions

Accurate C_p measurements of unstable quenched samples of monosulfide solid solutions support the hypothesis that the incompatibility in the magnetic ordering between end-member phases of FeS and NiS is the reason of instability of intermediate compositions. Heat capacity corresponds to 4.1 degrees of freedom for Fe-rich *mss* and 3.3 for Ni-rich ones. No exact limit between two types of magnetic ordering is there in the Fe/Ni ratio of *mss*, but rather transitional region where the fluctuations in magnetic properties manifest themselves in the irreproducibility of heat capacity.

End-member phases differ in magnetic ordering but identical in structure. As magnetic order is formed by interacting electrons, X-ray powder diffraction shows great changes in the intensity of reflections due to the changes in the electron density functions of 3*d*-atoms.

Acknowledgements

The research described in this publication was made possible in part by Award No. NO-008-X1 of the U.S. Civilian Research & Development Foundation for the Independent States of the Former Soviet Union (CRDF). The work was supported by RFBR grant 05-05-64556a.

References

1 V. A. Bryukvin, B. A. Fishman, V. A. Reznichenko, L. N. Shekhter, L. I. Blokhina and V. A. Kukoev, Russ. Metall., 4 (1987) 23.
2 O. A. Musbah and Y. A. Chang, Metall. Trans. A, 20 (1989) 1523.
3 E. F. Sinyakova, V. I. Kosyakov and V. A. Shestakov, Metall. Mater. Trans. B, 30 (1999) 715.
4 N. S. Gorbachev and A. N. Nekrasov, Dokl. Akad. Nauk, 399 (2004) 520.
5 L. N. Ertseva, O. N. Lukashevich, V. B. Starykh and L. Sh. Tsemekhman, Izvestia Akademii Nauk SSSR. Metally, 2 (1983) 3.
6 S.-J. Barnes, V. A. Melezhik and S. V. Sokolov, Can. Mineral., 39 (2001) 447.
7 A. E. Beswick, Economic Geology, 97 (2002) 1487.
8 E. F. Sinyakova, V. I. Kosyakov and B. G. Nenashev, Doklady Earth Sci., 397 (2004) 649.
9 V. A. Drebushchak, T. A. Kravchenko and V. S. Pavlyuchenko, J. Cryst. Growth, 193 (1998) 728.
10 V. A. Drebushchak, Zh. N. Fedorova and E. F. Sinyakova, J. Thermal Anal., 48 (1997) 727.
11 V. A. Drebushchak, E. V. Boldyreva, Yu. A. Kovalevskaya, I. E. Paukov and T. N. Drebushchak, J. Therm. Anal. Cal., 79 (2005) 65.
12 H. Saitoh, S. Ikeuchi and K. Saito, J. Therm. Anal. Cal., 81 (2005) 511.
13 S. P. Farrell and M. E. Fleet, Phys. Chem. Miner., 28 (2001) 17.
14 V. A. Drebushchak and T. A. Kravchenko, J. Therm. Anal. Cal., 56 (1999) 925.
15 F. Grønvold and S. Stølen, J. Chem. Thermodyn., 24 (1992) 913.
16 F. Grønvold, S. Stølen, A.K. Labban and E. F. Westrum, J. Chem. Thermodyn., 23 (1991) 261.
17 F. Grønvold and S. Stølen, Thermochim. Acta, 266 (1995) 213.
18 K. Basar, T. Shimoyama, D. Hosaka, Xianglian, T. Sakuma and M. Arai, J. Therm. Anal. Cal., 81 (2005) 507.

Received: January 2, 2006
Accepted: February 6, 2006
OnlineFirst: June 27, 2006

DOI: 10.1007/s10973-006-7501-x